AtDTX25, a member of the Multidrug And Toxic compound Extrusion family, is a vacuolar ascorbate transporter that controls intracellular iron cycling in Arabidopsis

Minh Thi Thanh Hoang, Minh Thi Thanh Hoang, Diego Almeida, Sandrine Chay, Carine Alcon, Claire Faillie, Catherine Curie, Stéphane Mari

HAL Id: hal-03258348
https://hal.inrae.fr/hal-03258348

Submitted on 1 Sep 2022

TASC1, a member of the Multidrug And Toxic compound Extrusion family, is a vacuolar ascorbate transporter that controls intracellular iron cycling in Arabidopsis

Journal:	*New Phytologist*
Manuscript ID	Draft
Manuscript Type:	MS - Regular Manuscript
Date Submitted by the Author:	n/a
Complete List of Authors:	Hoang, Minh; UNIVERSITY OF SIENCE, Department of Plant Biotechnology and Biotransformation Almeida, Diego; INRAE, BPMP Chay, Sandrine; INRAE, BPMP Alcon, Carine; CNRS, BPMP Corratge-Faillie, Claire; CNRS, BPMP Curie, Catherine; Institut National de la Recherche Agronomique, Université Montpellier II, Laboratoire de Biochimie et Physiologie Moléculaire des Plantes Mari, Stéphane; INRA Montpellier, UMR5004 Biochimie et Physiologie Moleculaire des Plantes AGRO-M/ INRA 2
Key Words:	iron, transport, vacuole, ascorbate, MATE transporter

SCHOLARONE™
Manuscripts

1   **TASC1, a member of the Multidrug And Toxic compound Extrusion family, is a vacuolar**

2   **ascorbate transporter that controls intracellular iron cycling in Arabidopsis**

3

4   **Minh Hoang*, Diego Almeida*, Sandrine Chay, Carine Alcon, Claire Faillie, Catherine Curie,**

5   **Stephane Mari**

6

7   BPMP, Univ Montpellier, CNRS, INRAE, Institut Agro, Montpellier, France

8

9   Author for correspondence:

10   Stephane Mari

11   stephane.mari@inrae.fr

12

13   * These authors contributed equally to this work

14

15   **Abstract**

16   - Iron (Fe) is an essential element, its transport is regulated by the cell redox balance. In

17   seeds, Fe enters the embryo as Fe^{2+} and is stored in vacuoles as Fe^{3+}. Through its ferric

18   reduction activity, ascorbate plays a major role in Fe redox state and hence Fe

19   transport within the seed.

20   - We have searched for ascorbate membrane transporters responsible for controlling

21   Fe reduction through a screening in the yeast ferric reductase-deficient *fre1* strain and

22   have isolated a member of the Multidrug And Toxic compound Extrusion (MATE)

23   family.

24   - TASC1 (for Transporter of ASCorbate 1) was shown to mediate ascorbate efflux when

25   expressed in yeast and Xenopus oocytes, in a pH-dependent manner. *In planta*, *TASC1*

26   is highly expressed during germination and encodes a vacuolar membrane protein.

27   Isolated vacuoles from a *tasc1-1* knockout mutant contained less ascorbate and more

28   Fe than WT and mutant seedlings were highly sensitive to Fe deficiency. Iron imaging

29   further showed that the remobilization of Fe from vacuoles was highly impaired in

30   mutant seedlings.

31   -   Taken together, our results establish TASC1 as a vacuolar ascorbate transporter,

32   required during germination to promote reduction of the pool of stored Fe^{3+} and its

33   remobilization to feed the developing seedling.

34

35

36

37   **Introduction**

38   Iron (Fe), the second most abundant metal of the Earth crust, is essential for life.

39   Chronologically, iron has been the first metal used by living organisms as a cofactor for a wide

40   range of biological processes such as molecular oxygen activation, reduction of

41   ribonucleotides, metabolism of peroxides and electron transfer reactions. Despite its

42   apparent abundance, Fe poses a real conundrum to all living organisms since environmental

43   Fe is found mostly as the poorly soluble (10^{-18}M), exchange-inert, Fe^{3+} form whereas the active

44   form, Fe^{2+}, has a strong pro-oxidant activity. Redox cycling between Fe^{2+} and Fe^{3+} is thus a

45   central process for the regulation of Fe uptake, storage and utilization. Most living organisms,

46   including mammals, plants and fungi, possess membrane-bound metal reductases belonging

47   to two major families, cytochrome b561 (mammals) and flavo-cytochromes (fungi, plants),

48   that play a crucial role in generating Fe^{2+} that is either readily transported by divalent metal

49   transporters or transferred to ferroxidase/permease transport systems (reviewed in (Kosman,

50   2010; Jain *et al.*, 2014)). At the intracellular level, storage and remobilization of Fe also rely on

51   redox cycling. The incorporation of excess Fe into ferritin protein complexes requires a

52   ferroxidation step catalyzed by ferritin itself whereas Fe release from these complexes

53   requires a one electron reduction step that is most probably mediated by physiological

54   reductants such as ascorbate (Watt *et al.*, 1988; Laulhere & Briat, 1993; De Domenico *et al.*,

55   2006; Melman *et al.*, 2013). Yeast cells, that do not produce ferritins, store Fe in the vacuole

56   as Fe^{3+}-(poly)-phosphate (Cockrell *et al.*, 2011; Park *et al.*, 2014) and the remobilization of this

57   pool is mediated by the lumen-oriented ferric reductase FRE6 that supplies Fe^{2+} either to the

58   ferrous efflux transporter Smf3p or to the ferroxidase/permease complex encoded by

59   Fet5p/Fthp (Singh *et al.*, 2007). In mature embryo of the model plant *Arabidopsis thaliana* Fe

60   is also stored as Fe^{3+} in vacuoles of specific cells surrounding the provascular strands (Lott &

61   West, 2001; Lanquar *et al.*, 2005; Kim *et al.*, 2006; Roschzttardtz *et al.*, 2009). Although the

62   overall mechanism of Fe retrieval from vacuoles remains uncharacterized, two divalent metal

63   transporters encoded by NRAMP3 and NRAMP4 play a key role in the efflux of Fe from

64   vacuoles during germination (Lanquar *et al.*, 2005), implying that, as shown in yeast, a

65   reduction step is likely to be required to generate Fe^{2+}, the *bona fide* substrate of NRAMP

66   proteins. Storage and remobilization of this particular Fe pool is crucial for the fate of the

67   future seedling since mutations in either the vacuolar influx transporter VIT1 or the efflux

68   transporters NRAMP3 and NRAMP4 severely compromises the growth of the seedling in Fe-

69   limiting conditions (Lanquar *et al.*, 2005; Kim *et al.*, 2006).

70   In plants, we have recently demonstrated that redox cycling of Fe is also crucial for the

71   transport between maternal tissues (seed coat) and the embryo. Indeed, isolated embryos

72   from Arabidopsis and pea exhibit high ferric reduction activity, necessary for Fe uptake, which

73   is not encoded by the expected membrane reductases of the FRO family. Instead, embryos

74   efflux massive amounts of ascorbate, which reduces Fe^{3+} ions that are delivered from the

75   maternal tissues as Fe-citrate-malate complexes (Grillet *et al.*, 2014). The association of

76   ascorbate-assisted reduction of Fe with transmembrane uptake of Fe^{2+} thus uncovered in

77   plants is reminiscent of the Fe uptake machinery described in human brain; indeed neuronal

78   cells take up Fe from Fe^{3+}-citrate complexes following a reduction step, which is catalyzed by

79   ascorbate released from these cells (Lane *et al.*, 2010). Taken together, these discoveries in

80   both animal and plant systems have shed a new light on Fe homeostasis, where ascorbate

81   efflux represents a new paradigm for ferric reduction and transport (Lane & Richardson,

82   2014).

83   Nevertheless, although ascorbate efflux activities have been reported in many instances, the

84   identity of the corresponding transport system remains elusive. To date, several plausible

85   candidates have been proposed, including exocytosis and/or plasma membrane anion

86   channels (reviewed in (Wilson, 2005)) however, no clear-cut demonstration of their identity

87   and function as ascorbate efflux transporters has been provided.

88   In the present work, we describe the isolation of an ascorbate efflux transporter that belongs

89   to the Multidrug And Toxic Compound Extrusion family (MATE). This transporter, named

90   *TASC1* (for Transporter of ASCorbate 1) was isolated through a yeast complementation

91   screening using the ferric reductase mutant *Δfre1*. We further show that *TASC1*, which

92   encodes a protein targeted to the vacuolar membrane in plant cells, is expressed in seeds and

93   most importantly during germination, where vacuolar Fe is crucial to sustain growth of the

94   developing seedling. Phenotypic analysis of plants mutated in *TASC1* further allowed

95   establishing that this protein plays a direct role in the redox cycling of Fe and its export from

96   the vacuole, a mechanism that is key to sustain growth of the developing seedling. Since MATE

97   are ubiquitous efflux transporters, these findings pave the way for future discoveries linking

98   ascorbate to Fe homeostasis in all living eukaryotic organisms.

99

100   **Materials and Methods**

101   **Yeast screening conditions.** The yeast mutant defective in the ferric reductase Fre1p (*Δfre1*,

102   *MATa*, *his3, leu2, met15, ura3, fre1::kanMX4)* was used in this work. Transformants were

103   grown on Yeast Nitrogen Base (YNB) medium supplemented with glucose (2% w/v), histidine,

104   leucine and methionine (50 µg.L^{-1}). Iron deficiency was induced by the addition of 75µM

105   bathophenanthroline disulfonate (BPDS). The screening media also contained 5mM of the

106   ascorbate precursor L-galactono-lactone (GL). The *Δfre1* cells were transformed with an

107   Arabidopsis cDNA library (Minet & Dufour, 1992) constructed in the pFL61 shuttle vector.

108   Clones growing in the YNB medium containing BPDS and GL were further selected for plasmid

109   extraction and sequencing.

110   **Measurement of ferric reduction activity.** To measure ferric reduction activity of the yeast

111   cells, the cells grown on medium with or without 10 mM L-GL overnight. Cell suspensions were

112   centrifuged and washed 3 times with sterilized water. The cells were then incubated in the

113   assay solution containing 5 mM MES buffer pH = 5.5, 300 µM (BPDS) and 100 µM Fe^{3+}-EDTA.

114   Fe reduction activity was monitored as the concentration of Fe^{2+}-BPDS$_3$

115   (bathophenanthrolinedisulfonate) complex formed in the assay solution by measuring

116   absorbance at 535 nm with a Hitachi U-2800spectrophotometer. OD535 was measured after

117   1 hour incubation in the dark at 22-25 °C with 250 RPM shaking.

118   **Heterologous expression of *TASC1* in *Xenopus laevis* oocytes and efflux activity assay.** The

119   *TASC1* coding region was cloned into modified pGEM-HE vector. cRNA were synthesized from

120   1 µg of linearized vector, *NheI*-digested, using the HiScribe™ T7 ARCA mRNA Kit with tailing

121   (NEB, http://www.NEB.com). Oocytes obtained surgically from benzocaine-anesthetized

122   *Xenopus laevis* were defolliculated using a 1 h collagenase-treatment under gentle shaking at

123   20°C in 25 ml of OR2 medium (NaCl 82,5mM, KCl 2mM, MgCl$_2$ 1 mM, HEPES-NaOH pH 7.4)

124   supplemented with 25 mg of collagenase (type IA, Sigma). Sorted stage V and VI oocytes were

125   then stored at 20°C in ND96 medium (NaCl 96mM, KCl 2mM, 1.8mM MgCl$_2$, CaCl$_2$ 1mM,

126   2.5mM Na-Pyruvate, HEPES-NaOH pH7.4) supplemented with 50 mg/ml gentamicin. Oocytes

127 were injected with 32 ng (50 nl) of *AtTasc1* cRNA using a micropipette (10–15 μm tip diameter)

128 and a pneumatic injector. After two days, *TASC1* cRNA injected oocytes and non-injected

129 oocytes (used as control) were transferred to fresh ND96 solution (pH 6.5) supplemented with

130 10 mM L-Ascorbic acid and injected with 25 nl of 100 mM ^{13}[C]-labeled L-Ascorbic acid (Sigma-

131 Aldrich, Ref. 795097, prepared in 100 mM Tris-MES pH 7.5). After 5 min of recovery, injected

132 oocytes were washed 5 times with ice-cold ND96 solution (pH 6.5), then placed for efflux

133 measurements by batches (n=3) of 10 oocytes into 2 ml vials at room temperature in ND96

134 medium. The requirement of a proton gradient was measured by incubations in different

135 ND96 set at different pH values (pH 5.5, 6.5 or 7.5) for 2 hrs. After incubation, 100 μl of ND96

136 medium from each batch were sampled in 3 replicates and dried. The ^{13}[C] abundance was

137 analyzed from sampled ND96 medium using an IsoPrime stable isotope analyzer Mass

138 Spectrometer (https://www.elementar.de).

139 **HPLC measurement of ascorbate.** For plant samples, material was collected, weighed and put

140 in the eppendorf tubes containing a plastic bead and stored in liquid nitrogen. Samples were

141 then ground and extracted with 5% (v/v) *o*-phosphoric acid. The homogenate was centrifuged

142 at 14000 rpm for 10 min at 4°C and the supernatant was collected and filtered for the analysis

143 of total ascorbate. Total ascorbate was determined after treatment with 2 mg/ml DTT for 25

144 min at room temperature in darkness. Isolated vacuoles were treated with phosphoric acid,

145 then vortexed vigorously and ascorbate concentration was measured by HPLC. The separation

146 was performed with isocratic elution using 0.1% TFA in water. The analyses were carried out

147 by injecting 10μL of samples onto a Nucleodur C18 column (particle size 5μm, pore size 100A)

148 connected to a Varian PrepStar pump using a flowrate of 0.7 mL.min^{-1}. Ascorbate was

149 detected using a UV-Visible spectrophotometric detector at 244nm and quantified with an

150 external standard calibration curve with pure ascorbate.

151 **Plant materials and growth conditions.** For soil-grown plants, seeds were stratified at 4°C for

152 2-3 days and sown onto the potting soil. Alternatively, 7-days old seedlings grown *in vitro* were

153 transferred into the soil. The greenhouse conditions for soil-grown plants were 16 hours light,

154 8 hours dark at 22°C and 70% humidity. For *in vitro* culture, after surface sterilization with 50%

155 ethanol, 12.5% bleach solution and 37.5% water for 10 min, seeds were rinsed three times

156 with 100% ethanol and stratified at 4°C for 2 days. For growth test on agar plates containing

157 different iron conditions, seeds were germinated on half strength MS. Iron sufficient medium

158 is half strength Murashige and Skoog (MS) medium containing 0.05% MES, 1% sucrose, 0.8%

159 agar and 50µM Fe^{3+}-citrate. The iron deficient medium is the same without Fe and a

160 supplement of 5 µM BPDS. For hydroponic cultures, 10-day-old plantlets were transferred

161 from half strength MS agar plates to *Arabidopsis* hydroponic solution (Hoagland solution-

162 appendix1). The hydroponic medium was renewed every 10 days. The growth chambers

163 conditions were 16 hour light/8 hour dark photoperiod at 21°C temperature and 65% the

164 relative humidity. The *tasc1-1* homozygous mutant line was isolated from GABI-Kat (GK_912H)

165 using the following primers EP16 (5'-TAAAAGTGGTGCTTGTGGTATCAG-3') and EP17 (5'-

166 AATAAATGAGTATTTTATTTGTAG-3'). Total RNA was extracted with Trizol and first strand cDNA

167 was synthesized with the RevertAid reverse transcription kit (Thermo Scientific). Full-length

168 *TASC1*   cDNA   was   amplified   by   RT-PCR   with   TASC1-FP   (5'-

169 GGAGATAGAACCATGAGTGGAGGTGGTGGAGA-3')   and   TASC1-RP   (5'-

170 TCCACCTCCGGATCCTCACTTTCTCTCTTCATCTCTTG-3'), *AtACT2* cDNA (actin 2, AT3G18780),

171 used   as   loading   control,   was   amplified   using   the   following   primers :   5'-

172 TGCTGTTGACTACGAGCAGG-3' and 5'-TCTGCTGGAATGTGCTGAGG-3'. The   search   for   putative

173 truncated versions of the full-length cDNA was realized using seven different reverse primers

174 hybridizing the end of the different exons, in order to amplify cDNA fragments of increasing

175 size up to the full-length version. The forward primers used were, respectively: rev1: 5'-

176 CCATAATACCGTAGATGAAGC-3' ;   rev2 :   5'-CAAAGCATGAAGCCGGAGGA-3';   rev3:   5'-

177 CATATGGAGAAAGCGGAAATTG-3';   rev4:   5'-CATGCTGCACCCATCAAGC-3';   rev5:   5'-

178   CCAGATAGAATGGGCTGGAT-3';   rev6:   5'-CCTTAATCCCAAAATTGAAAACG-3';   rev7:   5'-

179 TCACTTTCTCTCTTCATCTCTTG-3'.

180 **DNA cloning .** All cloning reactions were realized using the Gateway™ system (Invitrogen). All

181 *attB*-tailed PCR products were initially cloned into pDONR207 using BP Clonase, and their

182 sequence verified before subcloning into various plant expression vectors (using LR Clonase)

183 mentioned elsewhere. The cDNAs or promoter regions were amplified by a two step-PCR using

184 the high-fidelity Phusion polymerase (Thermo Scientific, Waltham, MA, USA) and the following

185 specific   primers   (At5g17700   FP,   5'-<u>GGAGATAGAACC</u>ATGAGTGGAGGTGGTGGAGA-3' ;

186 At5g17700 RP stop, 5'-<u>TCCACCTCCGGATCC</u>TCACTTTCTCTCTTCATCTCTTG-3' ; At5g17700 RP C-

187 ter,   5'-<u>TCCACCTCCGGATCC</u>CTTTCTCTCTTCATCTCTTG-3' ;   promoAt5g17700   FP,   5'-

188 <u>GGAGATAGAACC</u>   CAATAGTTTATGAGTTCATGCA-3' ;   promoAt5g17700   RP,   5'-

189 <u>TCCACCTCCGGATCC</u> TTTTCCTCTCTCTTTGATTTTC-3') containing universal Gateway attB1 and

190 universal Gateway attB2 sequences (underlined) for gateway recombination. For the TASC1-

191   GFP fusion, The *TASC1* cDNA was amplified without its stop codon and cloned into the pDONR

192   207 entry vector (Gateway; Invitrogen). *TASC1* cDNA was subsequently fused with GFP by

193   recombination with the destination vector pGWB5 to generate the C-terminal GFP fusion,

194   under the control of the CaMV *35S* promoter.

195   **Confocal microscopy.** For intracellular localization, the homozygous T2 transgenic plants were

196   imaged by confocal microscopy (Leica SP8) with laser excitation at 488 nm, emission light at

197   535 nm for GFP and laser excitation at 515 nm, emission light at 640-670 nm for FM4-64. Roots

198   of 10 day-old plantlets were mounted in water for microscopy observation or stained with 0.1

199   µg/ml FM4-64 for 5 minutes and washed twice in water before observation under the

200   microscope. For the fluorescent labelling of vacuoles, 10-day old seedlings were incubated

201   with Neutral Red (4 µM) for 20 minutes and signal was acquired at 500-540 nm with an

202   excitation at 561 nm.

203   **Glucuronidase histochemical staining.** Histochemical staining for GUS in transgenic

204   Arabidopsis plants was performed according to standard procedures with minor

205   modifications. Plant tissues at different development stages including germinating seeds,

206   seedlings, rosette leaves, flower and siliques were picked using clean forceps and immersed

207   in a X-Gluc stain solution (50 mM $NaPO_4$, 0.5 mM ferrocyanide, 0.5 mM ferricyanide, 0.05%

208   (v/v) Triton X-100, pH 7.2, and 1 mM 5-bromo-4-chloro-3-indolyl-β -D-glucuronide) overnight

209   at 37°C. For tissues containing chlorophyll, they were soaked in ethanol with 50%, 70%, 90%

210   and 100% successively until the samples were clear. For GUS histochemical staining in

211   embryos, embryos were fixed by 30 min of vacuum infiltration followed by 15 hour of soaking

212   in fixation solution containing 2% (w/v) paraformaldehyde, 1% (v/v) glutaraldehyde and 1%

213   (w/v) caffeine in 100 mM phosphate buffer (pH 7). Embryos were then dehydrated in

214   successive baths of 50%, 70%, 90%, 95% and 100% ethanol, butanol/ethanol 1:1 and 100%

215   butanol and embedded in the Technovit Resin according to the manufacturer's instructions.

216   Thin sections (4-6µm) were cut and observed under the microscope.

217   **Iron staining with the Perls/DAB procedure.** The staining protocol for Arabidopsis seedling

218   and histological sections described by Roschzttardtz et al. (2009) was followed.

219   **Vacuole isolation from leaves.** Vacuoles were isolated as described by Robert et al. (2007)

220   with some modifications. Firstly, to isolate mesophyll protoplasts, 2 g of rosette leaves from

221   30-day-old plants were collected and cut into small pieces. The processed leaves were floated

222   on protoplast enzyme solution (1% w/v cellulase, 1% w/v macerozyme, 0.4 % w/v $CaCl_2.2H_2O$

223   400 mM Mannitol and 10 mM MES pH6.0) and incubated in 4 hours with gentle shaking. The

224   released protoplasts were collected by centrifugation for 10 min at 19g and the pellets were

225   re-suspended in the washing buffer to remove hydrolytic enzymes. To isolate vacuoles, 12.5

226   ml of pre-warmed lysis buffer (0.2 M Mannitol, 10% v/v Ficoll, 10 µM EDTA pH=8, 5µM NaPO$_4$

227   pH 8.0 and 0.05% Neutral Red) were added to protoplast and re-suspended gently by pipetting

228   5-8 times and checking the protoplast disruption and vacuoles release under the light

229   microscope every 2 minutes. Vacuoles were then purified by overlaying with 6 ml 4 % (v/v)

230   Ficoll solution (mix 3 ml of lysis buffer and 4.5 ml of vacuole buffer : 450 mM mannitol, 5 µM

231   NaPO$_4$ pH 7.5, 2 µM EDTA pH 8.0), and addition of 2 ml of cold vacuole buffer on the top of

232   the gradient. After centrifugation for 50 min at 100000g at 10°C in Optima L-90K ultra-

233   centrifuge using slow acceleration and slow deceleration, the vacuoles were recovered from

234   the interface between middle and upper layers.

235   **Elemental analyses.** Shoots were collected and briefly rinsed with distilled water. Roots were

236   desorbed by washing for 10 min with 2mM CaSO4 and 10mM EDTA and for 3 min with 0.3

237   mM BPDS and 5.7 mM sodium dithionite and were then rinsed twice in deionized water.

238   Samples were dried at 80°C for 2 days. For mineralization, tissues were digested completely

239   in 70% (v/v) HNO$_3$ and 30% (v/v) H$_2$O$_2$ for 45 minutes at 180°C in a microwave (Berghof

240   speedwave digestion system). Elemental analysis was performed by Microwave Plasma-

241   Atomic Emission Spectrometer (MP-AES, Agilent) using calibration standard solutions

242   provided by the manufacturer.

243   **Data analysis.** All numerical values showed are means ± standard deviation, the number of

244   biological replicates is indicated as n. When the number of replicates was higher than 6,

245   statistical significance was tested using the Student's test, p values are indicated in the figure

246   legends. For experiments realized with a number of replicates lower than 6, the statistical

247   significance was tested with the Wilcoxon non parametric test.

248

249   **Results**

250

251   ***TASC1 mediates ascorbate transport in yeast cells and Xenopus oocytes***

252   Yeast complementation was used as a strategy to search for ascorbate (AsA) efflux

253   transporters from Arabidopsis. The yeast *Δfre1* strain, mutated in the major ferric chelate

254   reductase of the cell surface, is unable to acquire Fe in deficiency conditions and thus grows

255   poorly in Fe-limiting media (Georgatsou *et al.*, 1997). A cDNA library from *Arabidopsis thaliana*

256   was transformed in *Δfre1* with the idea that expression of a transporter able to mediate AsA

257   efflux in the medium should restore, at least in part, the ferric reduction capacity of the cell.

258   The growth medium was supplemented with L-galactono-lactone (GL), the biosynthetic

259   precursor that is readily converted in AsA by yeast cells that otherwise do not produce AsA

260   naturally (Berczi *et al.*, 2007). Among the positive clones picked for their restored growth on

261   Fe-limiting media, a clone expressing a cDNA coding for a member of the Multidrug And Toxic

262   Compound Extrusion family (MATE) was considered of high interest. Indeed, the hallmark of

263   the MATE proteins characterized so far is their capacity to mediate efflux of organic anions

264   such as organic acids and xenobiotics. According to the MATE nomenclature, this clone

265   corresponded to AtDTX25 (At5g17700) and was named TASC1, for Transporter of ASCorbate

266   1. Based on the ability of *TASC1* expression to restore growth of the *Δfre1* mutant (Fig. 1a) and

267   since this gene belongs to a family of *bona fide* efflux transporters, we then analyzed the

268   capacity of yeast cells to reduce Fe^{3+} through the efflux of AsA. The ferric reduction activity of

269   yeast cells was measured *in vitro* using the Fe^{2+} specific chromophore bathophenanthroline

270   disulfonic acid (BPDS). Cells expressing *TASC1* displayed a significant increase in ferric

271   reduction, compared to empty vector controls, specifically when cells had been pre-loaded

272   with the AsA precursor GL. This result indicated that the production of Fe^{2+} was mediated by

273   TASC1 and was ascorbate-dependent (Fig. 1b). We then analyzed the AsA efflux activity of

274   whole cells by measuring the concentration of AsA released in the medium, after preloading

275   cells with GL. In these conditions it was possible to show that cells expressing TASC1 were able

276   to efflux significant amounts of AsA in the medium within 3 hours, compared to empty vector

277   control cells (Fig. 1c). In order to further support these results with protein localization, we

278   also expressed an TASC1-GFP fusion in the yeast *Δfre1* strain. Depending on the level of

279   expression in the different clones, TASC1-GFP could be visualized at both the plasma

280   membrane and endomembranes including the vacuole (Fig. S1a) or only at the plasma

281   membrane (Fig. S1b). Drop tests further showed that this TASC1-GFP fusion was functional,

282   on the basis of the complementation of the growth defect of the *Δfre1* strain (Fig. S1e).

283   Further direct evidence of the ascorbate transport activity of TASC1 was obtained by

284   expressing *TASC1* in Xenopus oocytes. The release of ^{13}C in the medium was monitored from

285   oocytes previously injected with a 10mM ^{13}C-ascorbate solution over a four-hour period (Fig.

286   1d). A significant efflux of ascorbate could be detected from oocytes expressing TASC1 with a

287   progressive increase in the efflux activity over the 4-hour period tested. Based on this result,

288   we then tested the requirement of a proton gradient for the efflux activity of TASC1 by raising

289   the pH to 7.5. Compared to the efflux rate measured at pH5.5, incubating the oocytes at pH7.5

290   totally abolished ascorbate efflux, which indicates that TASC1 activity does require a proton

291   gradient. Taken together, these results strongly support the hypothesis that TASC1 is capable

292   of mediating transmembrane efflux of ascorbate from the cytosol. The dependency on a pH

293   gradient for the transport activity of TASC1 is an additional indication that this transport

294   activity corresponds to an antiport system that requires a proton gradient for the secondary

295   transport of ascorbate.

296

297   **TASC1 is a vacuolar transporter expressed during seed development and germination**

298   To determine the expression profile of *TASC1 in planta*, we examined the activity of 2 kb of its

299   promoter fused to the *uidA* reporter gene encoding the ß-glucuronidase (GUS). GUS activity

300   was observed in the seed *testa* (outer and inner integuments), seed endosperm, developing

301   embryo and in seedlings (Fig. 2a-c). *TASC1* promoter was also active in flowers, throughout

302   the developmental stages. In young flowers GUS activity could first be detected in the anthers,

303   anther filaments and in petals. The expression of TASC1 in petals increased with the age of

304   flowers (Fig. 2d).

305   The subcellular localization of TASC1 was then analyzed *in planta* by observing GFP

306   fluorescence of transgenic Arabidopsis plants expressing TASC1-GFP under the control of the

307   *CaMV 35S* promoter. Confocal microscopy analyses of root cells showed that the GFP

308   fluorescence did not co-localize with the plasma membrane marker FM4-64 (Fig. 3a). Instead,

309   the GFP signal was clearly observed on the membrane of a compartment occupying the vast

310   majority of the cell volume and depicting an invagination that is reminiscent of the localization

311   of the nucleus (Fig. 3a, arrowheads), these features corresponding to the vacuole. In order to

312   further confirm the tonoplastic localization of TASC1, we incubated TASC1-GFP seedlings with

313   Neutral Red, a dye used to stain the vacuoles of living cells. Besides being a chromophore,

314   Neutral Red can also be used as a fluorophore, that emits a red fluorescence when the

315   molecule is trapped in vacuoles (Dubrovsky *et al.*, 2006). The merging of TASC1-GFP and

316   Neutral Red signals clearly showed red fluorescent vacuoles surrounded by a green

317   fluorescent signal of TASC1-GFP, confirming that *in planta TASC1* is targeted to the tonoplast

318   and would therefore play a role at the level of the vacuole.

319

320 ***TASC1 regulates vacuolar Fe export***

321 In order to study the function of TASC1 *in planta*, we isolated a T-DNA mutant (*tasc1-1*) with

322 an insertion that was further located by sequencing in the last exon of the *TASC1* coding region

323 (Fig. S2a). Semi-quantitative reverse transcriptase amplification of the *TASC1* cDNA using

324 seven different reverse primers located at the end of the different exons of *TASC1* showed

325 that some truncated versions of the *TASC1* cDNA could be amplified, never beyond the sixth

326 exon (Fig. S2b). These truncated forms were still missing *ca* 40% of the full-length cDNA and it

327 was thus concluded that the *tasc1-1* mutation corresponded most likely to a knock-out allele

328 (Fig. S2b). To test the function of TASC1, we first focused on the growth of seedlings just after

329 germination. Indeed, during these early stages of growth, when *TASC1* is highly expressed, the

330 Fe pools stored in the vacuoles of the embryo are actively remobilized to feed the expanding

331 tissues, before the seedling reaches an autotrophic regime (Lanquar *et al.*, 2005). Therefore,

332 seeds of WT, *tasc1-1* and a TASC1-GFP complemented line were sown on standard (50 µM Fe-

333 citrate) and Fe deficient (no added Fe, supplemented with the Fe chelator BPDS) media and

334 grown for 7 days. Whereas no difference in growth was observed in Fe-replete condition,

335 *tasc1-1* seedlings appeared somewhat stunted in –Fe, with paler cotyledons and shorter roots,

336 compared to WT (Fig. 4a-b). This sensitivity of *tasc1-1* seedlings to Fe deficiency was alleviated

337 by the ectopic expression of a functional version of TASC1, indicating that the increased

338 sensitivity phenotype was indeed attributable to the inactivation of *TASC1* (Fig. 4a-b).

339

340 To analyze in more depth the effect of *TASC1* mutation on the fate of Fe pools during

341 germination and seedling growth, we monitored Fe remobilization from the vacuoles by

342 histochemical staining using the Perls/DAB procedure (Roschzttardtz *et al.*, 2009). Embryos

343 dissected from imbibed seeds of WT, *tasc1-1* mutant and complemented lines displayed

344 equivalent Fe staining (brown/black pigments) in the pro-vascular system of cotyledons and

345 hypocotyle (Fig. 5 upper lane). After 3 and 5 days of growth without Fe, in both WT and

346 complemented lines, Fe was completely remobilized since Fe was no more detectable in the

347 vasculature of cotyledons and hypocotyls (Fig. 5). In contrast, *tasc1-1* mutant seedlings

348 retained staining in the vascular system, mostly in the cotyledons (Fig. 5, arrowheads).

349 Histological analysis of Fe localization in thin sections of resin-embedded seedlings further

350 confirmed that Fe was indeed still visible in vacuoles of the *tasc1-1* mutant, whereas it had

351 completely disappeared in both WT and complemented line (Fig. 5, lower row, arrows). These

352 results indicated that in the *tasc1-1* mutant, the Fe remobilization process was strongly

353 affected, which could explain the reduced growth capacity of *tasc1-1* mutants in -Fe

354 conditions when seedlings strictly depend on this particular vacuolar Fe pool for their survival

355 and growth.

356

357 We next investigated whether impaired Fe remobilization from vacuoles of the *tasc1*-1 mutant

358 also occurred in older plants. When grown in Fe-deficient hydroponic condition during three

359 weeks, the growth of *tasc1-1* mutant plants was severely reduced, compared with WT and

360 complemented line (Fig. 6). Like for young seedlings, Perls-DAB staining on histological

361 sections of mature leaves showed the presence of Fe in the vacuoles of cells surrounding the

362 vascular system in *tasc1-1* (Fig. 7a, arrows), but not in WT and complemented line. This

363 observation therefore suggested that TASC1 function is not restricted to the early

364 development but also participates in Fe retrieval from vacuoles at different stages of plant

365 growth.

366 Taken together, our results strongly suggested that the function of TASC1 is to transport

367 ascorbate in vacuoles, in order to reduce Fe^{3+} and thus remobilize the Fe pools stored in these

368 vacuoles. To test this hypothesis, we isolated vacuoles from leaf protoplasts and quantified

369 metals (Fe, Zn, Mn) and ascorbate (Fig. 7b and c, respectively). Vacuoles of *tasc1-1* mutant

370 protoplasts contained 3 times more Fe than WT vacuoles, consistent with the Fe imaging

371 analyses. The concentration of other metals such as Zn and Mn remained similar between

372 *tasc1-1* and WT however. We therefore concluded that Fe is immobilized in the vacuoles of

373 the *tasc1-1* mutant. Contrary to Fe, ascorbate accumulated twice less in *tasc1-1* vacuoles

374 compared to WT (Fig. 7c), despite the fact that at the whole leaf level, both WT and *tasc1-1*

375 mutants did contain comparable amounts of ascorbate (Fig. S3). The concomitant increase of

376 Fe and decrease of ascorbate measured in *tasc1-1* vacuoles strongly suggested that

377 remobilization of vacuolar Fe requires the presence of ascorbate within the vacuole, which

378 itself likely relies on TASC1 ascorbate influx across the tonoplast. In this scenario, the inability

379 of *tasc1-1* cells to retrieve Fe from vacuoles would limit plant growth, reducing *in fine* its

380 tolerance to Fe deficiency.

381

382 **Discussion**

383 In the model plant *Arabidopsis thaliana*, the general mechanism of ionic Fe transport across

384 membranes, that is based on trans-membrane ferric reductases of the FRO family to generate

385 Fe^{2+}, has been recently challenged by the discovery of the role of ascorbate as an iron-reducing

386 molecule directly involved in the Fe transport process in seeds (Grillet *et al.*, 2014). This

387 finding, reminiscent of the Fe uptake from non-transferrin bound iron (NTBI) described in

388 human astrocyte cells (Lane *et al.*, 2010), represents a new mechanism to couple Fe reduction

389 with transmembrane transport at the surface of the embryo. Here, we show through the

390 characterization of the MATE transporter TASC1, that this mechanism also occurs at the

391 intracellular level, between the vacuolar lumen and the cytosol.

392 Indeed, we have demonstrated that TASC1, a tonoplast-targeted protein from Arabidopsis, is

393 competent in the transport of ascorbate when expressed in the yeast ferric reductase-

394 defective mutant *fre1* and in Xenopus oocytes. Moreover, in Arabidopsis, TASC1 participates

395 in the control of the efflux of Fe from the vacuole since we show that the *tasc1-1* mutant fails

396 to release Fe from vacuoles. MATE transporters mediate the secondary transport of a wide

397 variety of molecules such as nicotine, citrate, flavonoids, salicylic acid, protocatechuic acid and

398 abscisic acid (Takanashi *et al.*, 2014). Given the physiological importance of these molecules,

399 MATE transporters have emerged as important actors in some developmental processes such

400 as root development as well as in response to environmental stresses like aluminum toxicity

401 or iron and phosphorus translocation in deficiency conditions. Accordingly, MATE transporters

402 are generally classified based on the family of substrates transported or by the physiological

403 processes they are involved in. TASC1 could thus be part of the "Fe translocation" group of

404 MATE proteins, that includes the citrate transporter FRD3 and related proteins (Rogers &

405 Guerinot, 2002) and the protocatechuic acid transporters PEZ1 and PEZ2 (Bashir *et al.*, 2011;

406 Ishimaru *et al.*, 2011). Citrate efflux in the apoplast is crucial for the iron mobility between

407 cells that are symplastically disconnected, such as the root xylem parenchyma and pollen

408 grains (Roschzttardtz *et al.*, 2011). Likewise, in rice the efflux of protocatechuic acid in the

409 xylem sap plays a central role in the Fe deficiency response by increasing the solubilization of

410 precipitated Fe (Bashir *et al.*, 2011; Ishimaru *et al.*, 2011). Although TASC1 transport activity

411 can be linked with "Fe translocation", the nature of its substrate, ascorbate, represents an

412 entire new transport function, related but potentially not limited to Fe homeostasis.

413 Despite the fact that ascorbate is an essential molecule for plants that plays multiple roles in

414 many subcellular compartments, the only ascorbate transporter identified until now is

PHT4;4, a member of the PHosphate Transporter family (PHT) that mediates the influx of ascorbate in chloroplasts. The role of PHT4;4 is to fuel chloroplasts with ascorbate that is required as a co-substrate for enzymatic reactions of the non-photochemical quenching, the key metabolic responses of chloroplasts to high light stresses (Miyaji *et al.*, 2015).

Here, we have provided biochemical, physiological and genetic evidences, which together establish that TASC1 is a new ascorbate transporter in plants. Using yeast cells and oocytes as heterologous systems, we have shown that TASC1 has the capacity to mediate the efflux of ascorbate in the medium. Moreover, the ascorbate transport activity was shown to require a proton gradient as the driving force, suggesting that TASC1 may function as an ascorbate/H$^+$ antiporter, which is the typical transport signature of all the MATE transporters characterized so far (Takanashi *et al.*, 2014). The targeting of TASC1 at both the plasma membrane and the tonoplast in yeast cells, revealed by transport activity assays and confocal microscopy, should be taken with caution as it likely resulted from TASC1 being produced in a heterologous system. Actually, the overexpression of plant tonoplastic proteins in *Saccharomyces cerevisiae* often leads to a default targeting of a fraction of the molecules to the plasma membrane, thus explaining the complementation of a plasma membrane function by tonoplastic proteins. It is the case for NRAMP3 and NRAMP4, which despite being specifically targeted at the tonoplast in plants, were shown to efficiently complement the plasma membrane uptake systems Smf1p and Fet3p/Fet4p in yeast (Thomine *et al.*, 2000).

Our study has shed a new light on the role(s) of ascorbate in the vacuole. Compared to other organelles such as the chloroplast or the nucleus, the relative concentration of ascorbate reported in the vacuoles is unexpectedly low. Immunocytochemical studies have established that vacuoles contain no more than 3% of the total ascorbate labeling in cells (Zechmann *et al.*, 2011). However, upon high light stresses, the highest induction of ascorbate accumulation was observed in vacuoles, suggesting a role of this intracellular ascorbate pool in stress responses (Zechmann *et al.*, 2011). Given its high reactivity towards oxidizing molecules, the antioxidant activity of ascorbate will inevitably generate monodehydro-ascorbate (MDHA), the oxidized form of ascorbate. The classical regeneration of ascorbate from MDHA, known as the Foyer-Halliwell-Asada cycle, is not likely to take place in vacuoles since none of the enzymatic components of the cycle have been located in the vacuolar lumen. Instead, an alternative mechanism has been proposed to occur, specifically in vacuoles. This mechanism would involve transmembrane electron transfer proteins from the cytochrome b561 family

447   (Cyt-B) that are ubiquitous proteins, found in animal and plant phyla. The Cyt-B proteins

448   characterized so far were shown to use ascorbate as the electron donor, on the cytosolic side,

449   to catalyze a one-electron transfer to an acceptor that could be MDHA or ferric iron, on the

450   extra-cytosolic side (Berczi & Zimanyi, 2014; Lu *et al.*, 2014). Interestingly, several members

451   of the Cyt-B family have been identified as tonoplastic ascorbate-dependent oxido-reductases

452   in plants (Preger *et al.*, 2005; Berczi *et al.*, 2007).

453   Based on these findings and on our new results, it is possible that tonoplastic cytochrome

454   b561 would not be directly involved in Fe redox metabolism in the vacuole but rather in the

455   regeneration of ascorbate from MDHA that is produced as a result of Fe^{3+} reduction. This

456   mechanism would take place rapidly after germination to provide Fe to the developing plant.

457   Indeed, all the partners potentially required for this process, *AtTASC1*, *AtCYB1* and *AtCYB2*,

458   *AtNRAMP3* and *AtNRAMP4* are highly expressed in the vascular tissues after germination

459   (Verelst *et al.*, 2004; Lanquar *et al.*, 2005).

460   However, contrary to most of the genes involved in the response to Fe deficiency, the

461   expression of *TASC1* was not induced by Fe limitation (Fig. S4). Therefore, the regulation of

462   TASC1-mediated ascorbate-dependent Fe remobilization might occur at the level of ascorbate

463   itself. Indeed, Fe deficiency was shown to increase ascorbate accumulation in several plant

464   systems (Zaharieva & Abadia, 2003; Zaharieva *et al.*, 2004; Urzica *et al.*, 2012), through the

465   induction of genes involved in ascorbate biosynthesis (*VTC2*) and recycling (*MDAR1*) (Urzica

466   *et al.*, 2012). The rapid adjustments in ascorbate concentration might thus be more efficient

467   to cope with fluctuations of Fe status than changes in *TASC1* expression. In terms of expression

468   profile, *TASC1* and the citrate effluxer *FRD3* display some overlap, since both genes are

469   expressed in the embryo and integument of the developing seed, in young seedlings and in

470   anthers (Roschzttardtz *et al.*, 2011). This overlap in expression profile could be an indication

471   that both transport activities, and therefore both ascorbate and citrate, are required for the

472   movement of Fe between symplastically disconnected cells, as previously reported for FRD3

473   (Roschzttardtz *et al.*, 2011). Such a mechanism where citrate and ascorbate act together for

474   Fe translocation is reminiscent of the Fe trafficking in the brain where Fe-citrate (generally

475   referred to as non-transferrin-bound iron) is reduced by ascorbate into Fe^{2+} that is then

476   imported by transporters of the NRAMP family (Moos *et al.*, 2007; Lane & Lawen, 2008; Lane

477   & Richardson, 2014).

478   In the proposed mechanism of Fe remobilization from vacuoles, it is assumed that Fe is stored

479   in vacuoles under its oxidized form. Although the speciation of Fe in vacuoles has never been

480   fully addressed, several experimental evidences support this hypothesis and thus the need for

481   a reduction step during its remobilization. First, this vacuolar Fe pool in embryos reacts with

482   ferrocyanide, an iron dye that is specific for Fe^{3+} (Roschzttardtz *et al.*, 2009). Second, during

483   seed maturation, the ascorbate concentration drops, reaching undetectable levels in dry

484   seeds (Gest *et al.*, 2013). This will generate a pro-oxidant state, in favor of the accumulation

485   of the oxidized ferric form over the ferrous. Finally, it was shown that iron and phosphorus co-

486   localize in specific structures in vacuoles, the globoids (Lanquar *et al.*, 2005) that are known

487   to accumulate phosphorus under the form of phytate (Lott & West, 2001), which is a highly

488   efficient ligand of Fe^{3+} (Veiga *et al.*, 2015). Actually, the affinity of phytate (inositol-hexakis-

489   phosphate, InsP6) for Fe^{3+} is at least 10 orders of magnitude higher than for Fe^{2+} (Veiga *et al.*,

490   2015). Moreover, this preferential binding to Fe^{3+} is strongly increased in acidic conditions

491   since it has been shown, *in vitro*, that below pH5 the InsP6-Fe^{2+} complexes totally dissociate

492   whereas almost 100% of Fe^{3+} will remain bound to InsP6 (Veiga *et al.*, 2015). Therefore, from

493   a biological point of view, the acidification of the vacuolar lumen that takes place during

494   germination (Maeshima *et al.*, 1994; Bolte *et al.*, 2011; Wilson *et al.*, 2016) will be necessary

495   but not sufficient to dissociate Fe^{3+} from phytate. The drop in pH has thus to be accompanied

496   by a reduction step in order to dissociate Fe from its ligand and generate the more mobile Fe^{2+}

497   form that will be readily transported out of the vacuole by the divalent metal transporters

498   NRAMP3 and NRAMP4 (Lanquar *et al.*, 2005).

499   In conclusion, we have identified a new ascorbate transporter in the vacuolar membrane,

500   belonging to the MATE family, that plays an important role in the process of Fe remobilization

501   in embryos during germination. The characterization of this new transporter has shed a new

502   light on the role of ascorbate, the main anti-oxidant molecule in plant cells, in Fe homeostasis.

503   Our work has contributed to add a new brick to the complex mechanism by which iron, stored

504   in vacuoles in Arabidopsis embryos, is remobilized to feed the developing seedling. In

505   conditions of Fe deficiency, TASC1-mediated ascorbate transport appears to be as crucial as

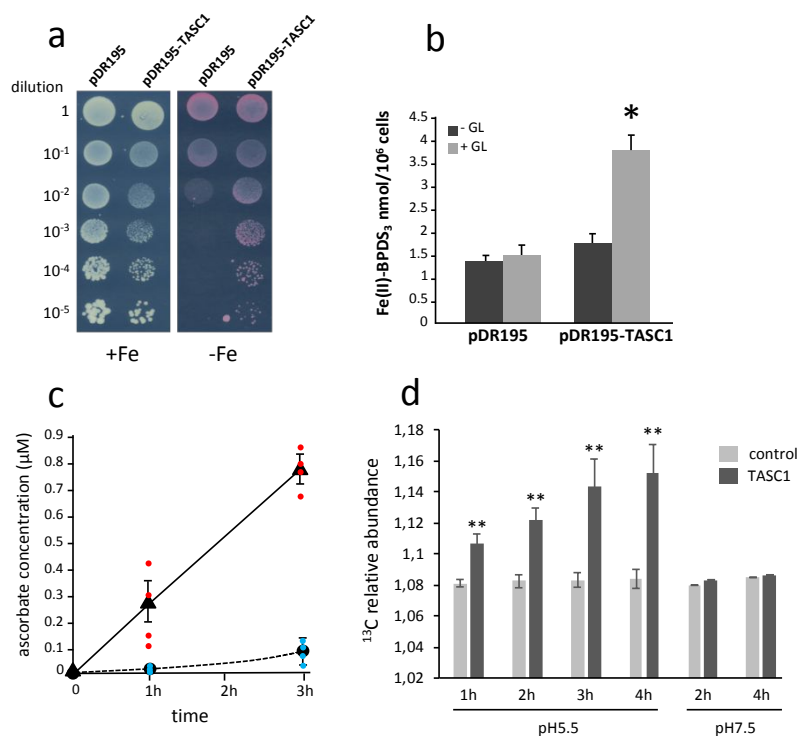506   NRAMP3 and NRAMP4 for the overall remobilization process.

507

508   **Acknowledgements**

512

513

514

515

516

517 **Figure 1. Isolation and characterization of TASC1, an ascorbate efflux transporter.** (A) *Δfre1*

518 mutant yeast was transformed with empty vector (pDR195) or with the vector expressing

519 *TASC1* (pDR195-TASC1). Serial dilutions of an OD=1 initial culture were plated on YNB media

520 supplemented with 5 mM GL and either Fe (+Fe) or no Fe (-Fe) obtained by the addition of 75

521 μM BPDS. (B) Ferric reduction activity of whole yeast cells. Transformants were grown

522 overnight in YNB with (grey bars) or without (black bars) 10 mM GL and ferric reduction

523 activity was measured. Data are means ± SD of n=3 independent clones, * P<0.01, Wilcoxon

524 test. (C) Ascorbate efflux in the medium from whole cells that had been grown overnight in

525 the presence of 10 mM GL. Ascorbate concentration in the medium was measured by HPLC.

526 Data are means ± SD, n=4 independent clones. (D) Time course of ^{13}C-ascorbate efflux from

527 *Xenopus* oocytes expressing TASC1, measured at pH5.5 or pH7.5. Data are means ± SD, n=4

528 independent sets containing 10 oocytes per condition, ** indicates a significant difference

529 from control using the t-test, P<0.01%.

530

531

532

533
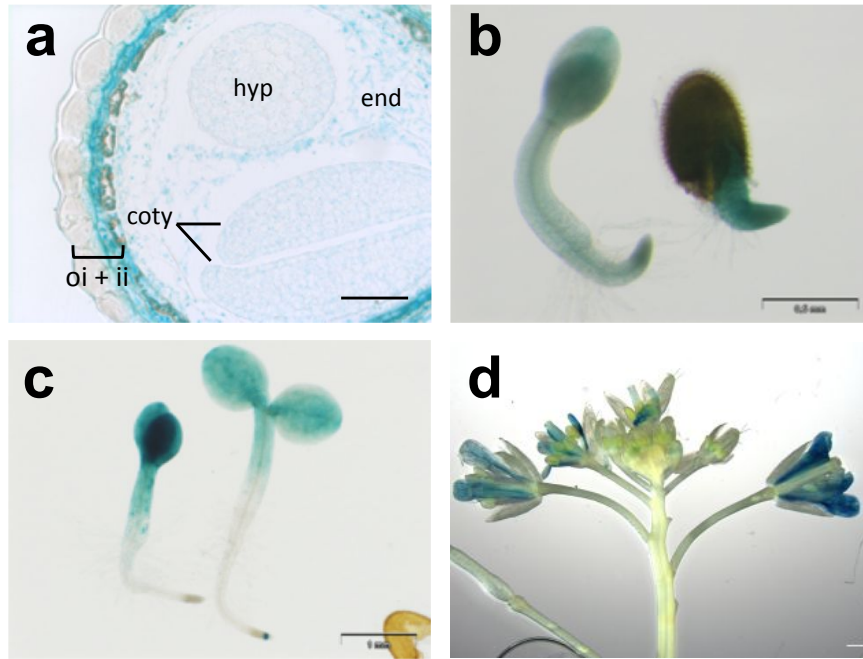
Figure 2. *TASC1* is expressed in flowers, seeds and seedlings. Histochemical staining of GUS activity in a transgenic plant expressing the *TASC1* promoter-GUS fusion. (a) Seed cross section at mature green embryo stage, (b-c) seedlings, 1-2 (B) and 4 (c) days after imbibition, (d) GUS staining of a whole flower bud; oi=outer integument, ii=inner integument, end=endosperm, hyp=embryo hypocotyl, coty=embryo cotyledons. (D)
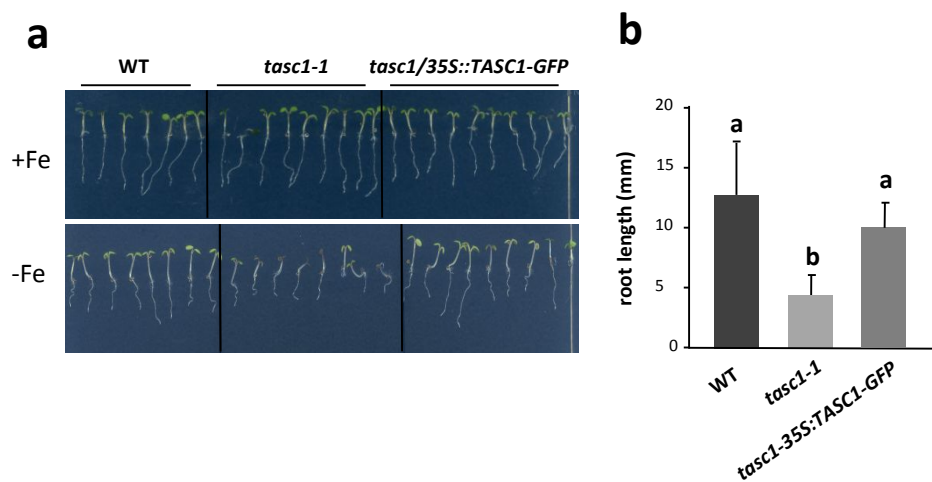
539

540
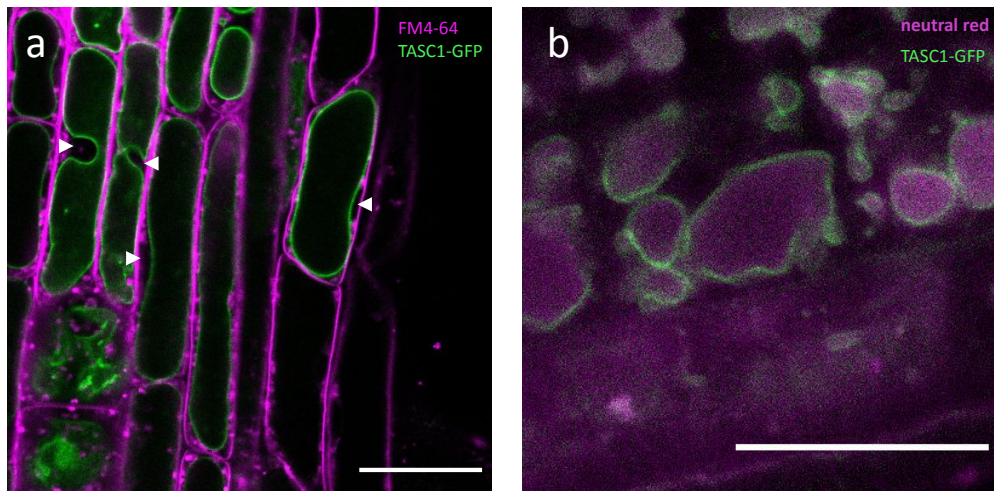
Figure 3. TASC1 is a tonoplastic protein. Confocal microscopy of roots from 1 week-old *tasc1-1* seedlings expressing TASC1-GFP (green) fusion. (a) Plasma membrane was stained with FM4-64 (magenta), (b) vacuoles were stained with Neutral Red (magenta). Arrowheads indicate invaginations of the tonoplast surrounding the nucleus. bar = 10µm.

545

546

547 **Figure 4. TASC1 is required for seedling growth in Fe deficiency.** (A) *tasc1-1* mutants are

548 sensitive to Fe deficiency. Seedlings were grown for 5 days in standard (50µM Fe-citrate, +Fe)

549 or deficiency (no Fe added, 50µM BPDS, -Fe) Fe condition. (B) primary root length of seedlings

550 grown in –Fe. Data are means ± SD, n=10 seedlings per genotype, different letters indicate

551 significant differences by Student's *t*-test, P<0.01.

552
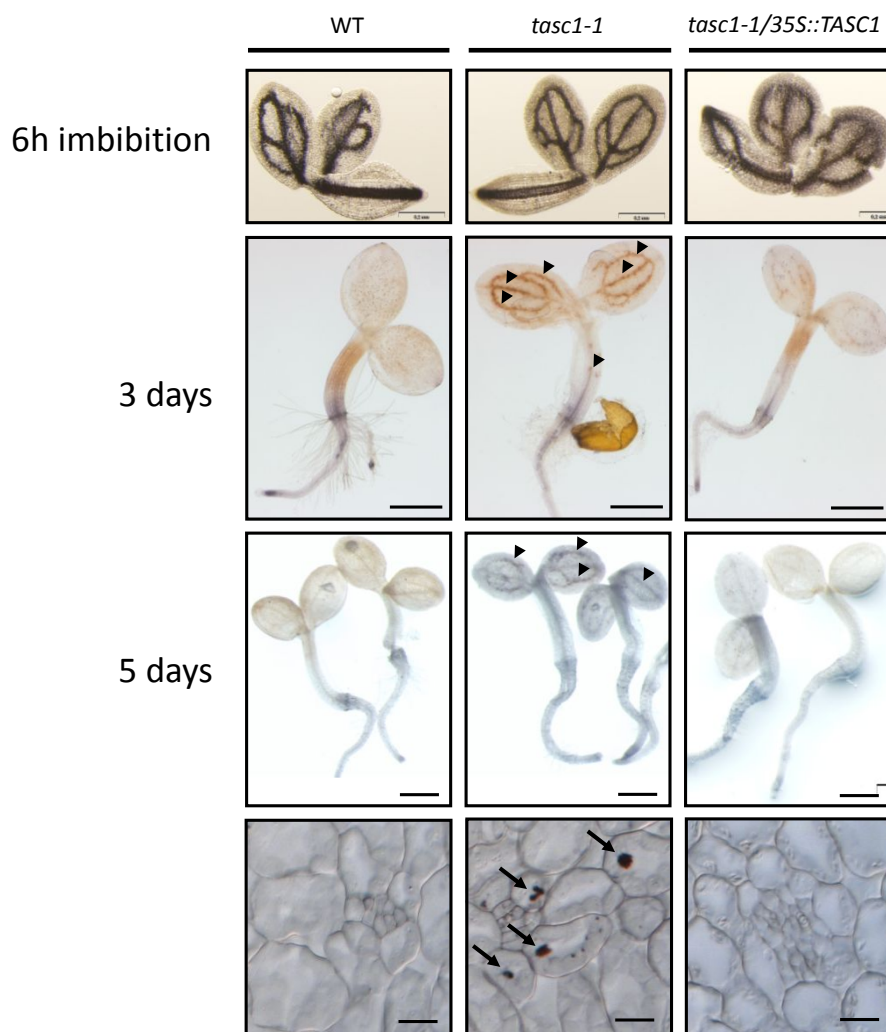
Figure 5. TASC1 participates in the remobilization of Fe during germination. Histochemical staining of Fe with the Perls/DAB procedure on embryos dissected from imbibed seeds (upper lane) 3- and 5-day old seedlings grown without Fe were stained for Fe (brown coloration in the vascular system, indicated by arrowheads), bar=0.5 mm. Lower lane, Perls/DAB staining of Fe on ultra-thin sections of cotyledons, Fe is visible as brown deposits in the vacuoles (arrows), bar=50μm.

561
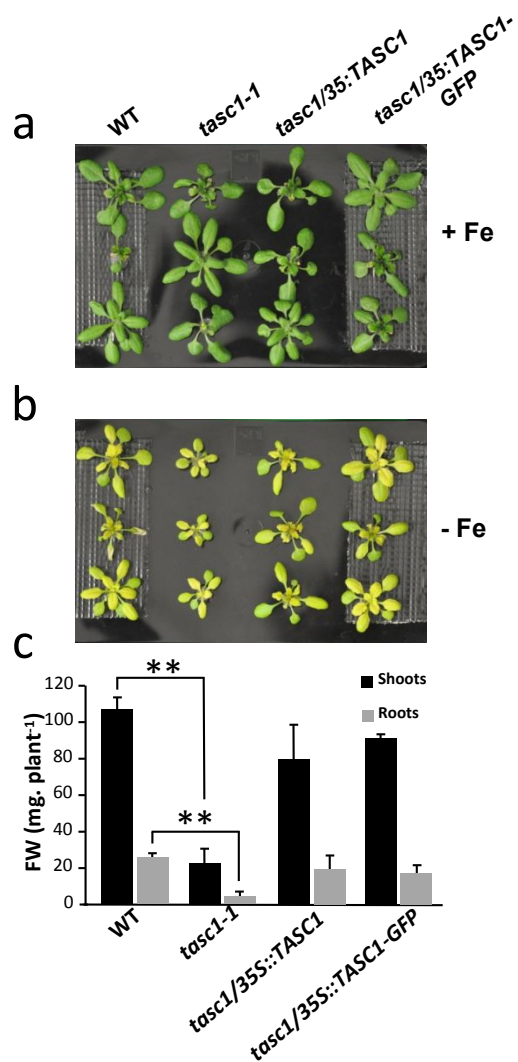
Figure 6. TASC1 is involved in the tolerance to Fe deficiency. Ten day-old seedlings were transferred in hydroponic conditions and grown for 2 weeks in standard (+Fe, 10µM Fe-citrate) or Fe deficient (-Fe, no Fe added). Lower panel, biomass quantification of plants grown on – Fe. Data are means ± SD, n=12 plants per genotype, ** indicate significant differences with Student's test, P<0.01.

567
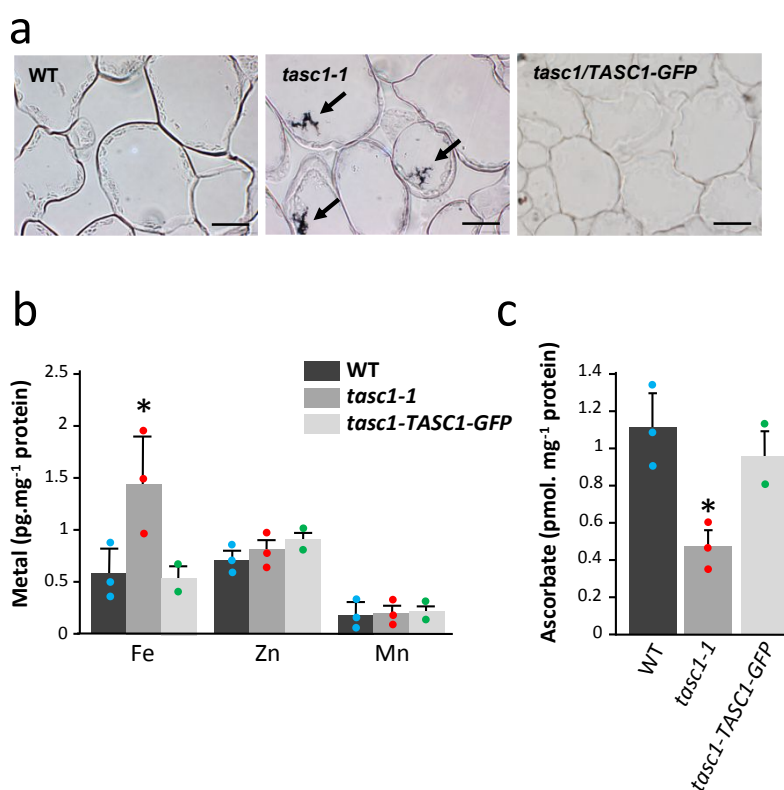
568

569

570 **Figure 7. Vacuolar Fe remobilization depends on TASC1-mediated ascorbate transport.** (A)

571 Perls/DAB staining of Fe on ultra-thin sections of leaves from 3-week-old plants grown in

572 hydroponic condition. Arrows indicate Fe depositions in vacuoles of mesophyll cells

573 (bar=20μm). (B, C) metals and ascorbate quantification, respectively, from vacuoles isolated

574 from leaf protoplasts of plants grown in +Fe. Data are means±SE of n=3 independent

575 preparations, * indicate statistical difference with Wilcoxon test, P<0.1.

576

577

578

Bashir K, Ishimaru Y, Shimo H, Kakei Y, Senoura T, Takahashi R, Sato Y, Sato Y, Uozumi N, Nakanishi H, et al. 2011. Rice phenolics efflux transporter 2 (PEZ2) plays an important role in solubilizing apoplasmic iron. *Soil Science and Plant Nutrition* **57**(6): 803-812.

Berczi A, Su D, Asard H. 2007. An Arabidopsis cytochrome b561 with trans-membrane ferrireductase capability. *Febs Letters* **581**(7): 1505-1508.

Berczi A, Zimanyi L. 2014. The Trans-Membrane Cytochrome b561 Proteins: Structural Information and Biological Function. *Current Protein & Peptide Science* **15**(8): 745-760.

Bolte S, Lanquar V, Soler MN, Beebo A, Satiat-Jeunemaitre B, Bouhidel K, Thomine S. 2011. Distinct Lytic Vacuolar Compartments are Embedded Inside the Protein Storage Vacuole of Dry and Germinating Arabidopsis thaliana Seeds. *Plant and Cell Physiology* **52**(7): 1142-1152.

Cockrell AL, Holmes-Hampton GP, McCormick SP, Chakrabarti M, Lindahl PA. 2011. Mossbauer and EPR Study of Iron in Vacuoles from Fermenting Saccharomyces cerevisiae. *Biochemistry* **50**(47): 10275-10283.

De Domenico I, Vaughn MB, Li LT, Bagley D, Musci G, Ward DM, Kaplan J. 2006. Ferroportin-mediated mobilization of ferritin iron precedes ferritin degradation by the proteasome. *Embo Journal* **25**(22): 5396-5404.

Dubrovsky JG, Guttenberger M, Saralegui A, Napsucialy-Mendivil S, Voigt B, Baluska F, Menzel D. 2006. Neutral red as a probe for confocal laser scanning microscopy studies of plant roots. *Annals of Botany* **97**(6): 1127-1138.

Georgatsou E, Mavrogiannis LA, Fragiadakis GS, Alexandraki D. 1997. The yeast Fre1p/Fre2p cupric reductases facilitate copper uptake and are regulated by the copper-modulated Mac1p activator. *J Biol Chem* **272**(21): 13786-13792.

Gest N, Gautier H, Stevens R. 2013. Ascorbate as seen through plant evolution: the rise of a successful molecule? *Journal of Experimental Botany* **64**(1): 33-53.

Grillet L, Ouerdane L, Flis P, Hoang MTT, Isaure M-P, Lobinski R, Curie C, Mari S. 2014. Ascorbate efflux as a new strategy for iron reduction and transport in plants. *The Journal of biological chemistry* **289**(5): 2515-2525.

Ishimaru Y, Kakei Y, Shimo H, Bashir K, Sato Y, Uozumi N, Nakanishi H, Nishizawa NK. 2011. A Rice Phenolic Efflux Transporter Is Essential for Solubilizing Precipitated Apoplasmic Iron in the Plant Stele. *Journal of Biological Chemistry* **286**(28): 24649-24655.

Jain A, Wilson GT, Connolly EL. 2014. The diverse roles of FRO family metalloreductases in iron and copper homeostasis. *Frontiers in Plant Science* **5**.

Kim SA, Punshon T, Lanzirotti A, Li L, Alonso JM, Ecker JR, Kaplan J, Guerinot ML. 2006. Localization of iron in Arabidopsis seed requires the vacuolar membrane transporter VIT1. *Science* **314**(5803): 1295-1298.

Kosman DJ. 2010. Redox Cycling in Iron Uptake, Efflux, and Trafficking. *Journal of Biological Chemistry* **285**(35): 26729-26735.

Lane DJR, Lawen A. 2008. Non-transferrin iron reduction and uptake are regulated by transmembrane ascorbate cycling in K562 cells. *Journal of Biological Chemistry* **283**(19): 12701-12708.

Lane DJR, Richardson DR. 2014. The active role of vitamin C in mammalian iron metabolism: Much more than just enhanced iron absorption! *Free Radical Biology and Medicine* **75**: 69-83.

Lane DJR, Robinson SR, Czerwinska H, Bishop GM, Lawen A. 2010. Two routes of iron accumulation in astrocytes: ascorbate-dependent ferrous iron uptake via the divalent

625   metal transporter (DMT1) plus an independent route for ferric iron. *Biochemical*
626   *Journal* **432**: 123-132.

627   **Lanquar V, Lelievre F, Bolte S, Hames C, Alcon C, Neumann D, Vansuyt G, Curie C, Schroder**
628   **A, Kramer U, et al. 2005.** Mobilization of vacuolar iron by AtNRAMP3 and AtNRAMP4
629   is essential for seed germination on low iron. *Embo J* **24**(23): 4041-4051.

630   **Laulhere JP, Briat JF. 1993.** Iron release and uptake by plant ferritin: effects of pH, reduction
631   and chelation. *Biochemical Journal* **290**(Pt 3): 693-699.

632   **Lott JNA, West MM. 2001.** Elements present in mineral nutrient reserves in dry Arabidopsis
633   thaliana seeds of wild type and pho1, pho2, and man1 mutants. *Canadian Journal of*
634   *Botany-Revue Canadienne De Botanique* **79**(11): 1292-1296.

635   **Lu PL, Ma D, Yan CY, Gong XQ, Du MJ, Shi YG. 2014.** Structure and mechanism of a eukaryotic
636   transmembrane ascorbate-dependent oxidoreductase. *Proceedings of the National*
637   *Academy of Sciences of the United States of America* **111**(5): 1813-1818.

638   **Maeshima M, Haranishimura I, Takeuchi Y, Nishimura M. 1994.** ACCUMULATION OF
639   VACUOLAR H+-PYROPHOSPHATASE AND H+-ATPASE DURING REFORMATION OF THE
640   CENTRAL VACUOLE IN GERMINATING PUMPKIN SEEDS. *Plant Physiology* **106**(1): 61-69.

641   **Melman G, Bou-Abdallah F, Vane E, Maura P, Arosio P, Melman A. 2013.** Iron release from
642   ferritin by flavin nucleotides. *Biochimica Et Biophysica Acta-General Subjects* **1830**(10):
643   4669-4674.

644   **Miyaji T, Kuromori T, Takeuchi Y, Yamaji N, Yokosho K, Shimazawa A, Sugimoto E, Omote H,**
645   **Ma JF, Shinozaki K, et al. 2015.** AtPHT4;4 is a chloroplast-localized ascorbate
646   transporter in Arabidopsis. *Nature Communications* **6**.

647   **Moos T, Nielsen TR, Skjorringe T, Morgan EH. 2007.** Iron trafficking inside the brain. *Journal*
648   *of Neurochemistry* **103**(5): 1730-1740.

649   **Park J, McCormick SP, Cockrell AL, Chakrabarti M, Lindahl PA. 2014.** High-Spin Ferric Ions in
650   Saccharomyces cerevisiae Vacuoles Are Reduced to the Ferrous State during Adenine-
651   Precursor Detoxification. *Biochemistry* **53**(24): 3940-3951.

652   **Preger V, Scagliarini S, Pupillo P, Trost P. 2005.** Identification of an ascorbate-dependent
653   cytochrome b of the tonoplast membrane sharing biochemical features with members
654   of the cytochrome b561 family. *Planta* **220**(3): 365-375.

655   **Rogers EE, Guerinot ML. 2002.** FRD3, a Member of the Multidrug and Toxin Efflux Family,
656   Controls Iron Deficiency Responses in Arabidopsis. *Plant Cell* **14**(8): 1787-1799.

657   **Roschzttardtz H, Conejero G, Curie C, Mari S. 2009.** Identification of the Endodermal Vacuole
658   as the Iron Storage Compartment in the Arabidopsis Embryo. *Plant Physiology* **151**(3):
659   1329-1338.

660   **Roschzttardtz H, Seguela-Arnaud M, Briat JF, Vert G, Curie C. 2011.** The FRD3 Citrate Effluxer
661   Promotes Iron Nutrition between Symplastically Disconnected Tissues throughout
662   Arabidopsis Development. *Plant Cell* **23**(7): 2725-2737.

663   **Singh A, Kaur N, Kosman DJ. 2007.** The metalloreductase Fre6p in Fe-efflux from the yeast
664   vacuole. *J Biol Chem* **282**(39): 28619-28626.

665   **Takanashi K, Shitan N, Yazaki K. 2014.** The multidrug and toxic compound extrusion (MATE)
666   family in plants. *Plant Biotechnology* **31**(5): 417-430.

667   **Thomine S, Wang R, Ward JM, Crawford NM, Schroeder JI. 2000.** Cadmium and iron transport
668   by members of a plant metal transporter family in Arabidopsis with homology to
669   Nramp genes. *Proc. Natl Acad. Sci. U. S. A.* **97**(9): 4991-4996.

670   **Urzica EI, Casero D, Yamasaki H, Hsieh SI, Adler LN, Karpowicz SJ, Blaby-Haas CE, Clarke SG,**
671   **Loo JA, Pellegrini M, et al. 2012.** Systems and Trans-System Level Analysis Identifies

672   Conserved Iron Deficiency Responses in the Plant Lineage. *Plant Cell* **24**(10): 3921-
673   3948.
674 **Veiga N, Macho I, Gomez K, Gonzalez G, Kremer C, Torres J. 2015.** Potentiometric and
675   spectroscopic study of the interaction of 3d transition metal ions with inositol
676   hexakisphosphate. *Journal of Molecular Structure* **1098**: 55-65.
677 **Verelst W, Kapila J, Engler JD, Stone JM, Caubergs R, Asard H. 2004.** Tissue-specific expression
678   and developmental regulation of cytochrome b561 genes in Arabidopsis thaliana and
679   Raphanus sativus. *Physiologia Plantarum* **120**(2): 312-318.
680 **Watt GD, Jacobs D, Frankel RB. 1988.** REDOX REACTIVITY OF BACTERIAL AND MAMMALIAN
681   FERRITIN - IS REDUCTANT ENTRY INTO THE FERRITIN INTERIOR A NECESSARY STEP FOR
682   IRON RELEASE. *Proceedings of the National Academy of Sciences of the United States*
683   *of America* **85**(20): 7457-7461.
684 **Wilson JX 2005.** Regulation of vitamin C transport. *Annual Review of Nutrition*, 105-125.
685 **Wilson KA, Chavda BJ, Pierre-Louis G, Quinn A, Tan-Wilson A. 2016.** Role of vacuolar
686   membrane proton pumps in the acidification of protein storage vacuoles following
687   germination. *Plant Physiology and Biochemistry* **104**: 242-249.
688 **Zaharieva TB, Abadia J. 2003.** Iron deficiency enhances the levels of ascorbate, glutathione,
689   and related enzymes in sugar beet roots. *Protoplasma* **221**(3-4): 269-275.
690 **Zaharieva TB, Gogorcena Y, Abadia J. 2004.** Dynamics of metabolic responses to iron
691   deficiency in sugar beet roots. *Plant Science* **166**(4): 1045-1050.
692 **Zechmann B, Stumpe M, Mauch F. 2011.** Immunocytochemical determination of the
693   subcellular distribution of ascorbate in plants. *Planta* **233**(1): 1-12.
694